5th International Conference on Computational and Mathematical Biomedical Engineering – CMBE2017
10-12 April 2017, United States
P. Nithiarasu, A.M. Robertson (Eds.)

A COMPUTATIONAL CASE STUDY FOR THE TREATMENT OF HEAD-AND-NECK TUMOR USING INTERSTITIAL PHOTODYNAMIC THERAPY

Ye Han[1,*], Emily Oakley[2], Gal Shafirstein[2], Yoed Rabin[1], Levent Burak Kara[1]
[1] Department of Mechanical Engineering, Carnegie Mellon University, Pittsburgh, PA, 15213, USA,
[2] Photodynamic Therapy Center, Department of Cell Stress Biology, Roswell Park Cancer Institute, Buffalo, NY, 14263,USA ; * yehan@andrew.cmu.edu

SUMMARY

In interstitial photodynamic therapy (I-PDT), image-based preplanning is employed to compute optimal laser fiber configuration on complex tumor shape. Unfortunately, tumor deformation during the I-PDT procedure may have negative impact on the actual light dose delivery. This paper presents a case study of locally advanced head-and-neck cancer (LAHNC). Light propagation modeling on the non-deformed and deformed LAHNC is used to characterize the potential treatment degradation due to tumor deformation. A computational method of calculating deformed tumor shape by tracking implanted fiducial markers is described, which helps bridge the gap between geometric model in preplanning and actual deformed shape.

Key words: *interstitial photodynamic therapy, head-and-neck cancer, tumor deformation, shape reconstruction*

1 INTRODUCTION

Interstitial photodynamic therapy (I-PDT) has been shown promising results in the treatment of locally advanced head-and-neck cancer (LAHNC). In this therapy modality, a light sensitive drug is systemically administrated, after which multiple laser fibers are inserted to illuminate target regions. During the I-PDT preplanning phase, computed tomography (CT) is initially used to reconstruct digital LAHNC model. Based on the reconstructed model, optimal configuration of laser fibers is computed with light propagation modeling. However, treatment failure could occur at the margins of the tumor due to the mismatch between the original reconstruction and the actually deformed shape during operation.

This study presents a computational case study for a CT reconstructed LAHNC model in I-PDT. First, light propagation modeling is utilized to characterize possible defect caused by tumor shape deformation during I-PDT procedure. Defect in this context is defined as the difference between the deformed and non-deformed tumor volumes that receive a prescribed light dose. Second, a novel computational method designed for calculating deformed tumor shape is described. The new method uses input of two sources: (i) the pre-deformed tumor shape and (ii) displaced position of implanted fiducial markers (FM) during therapy. The computation process takes only a few seconds, which allows for real time update of the treatment planning.

Results of this study demonstrate a prediction error of less than 1mm, which is the typical uncertainty of distance measurement in high-quality ultrasound imaging and CT imaging. The computational efficiency of presented method further demonstrates its potential in clinical application.

2 METHODOLOGY

2.1 Light propagation modeling

The finite element model (FEM) for computing the light propagation was described previously in [1]. In this approach, light propagation is modeled as a transient and three-dimensional (3-D) diffusion problem [2,3]:

$$\frac{1}{c_n}\left(\frac{\partial}{\partial t}\Phi(x,\,y,\,z,\,t)\;-\;\nabla\left(\alpha^n\nabla\Phi(x,\,y,\,z,\,t)\right)\right)=-\mu_a^n\Phi(x,\,y,\,z,\,t) \tag{1}$$

$$\alpha^n=\;c_n\cdot[3(\mu_a^n+(1-g)\mu_s^n)]^{-1} \tag{2}$$

where $\Phi(x,\,y,\,z,\,t)$ is the photon flux (Photons/m²/sec), α^n is the optical diffusion coefficient (m²/sec) of tissue constituent n, μ_a^n and μ_s^n are the linear absorption and scattering coefficients (1/m), g is the optical anisotropy factor, and c_n is the speed of light in the tissue.

2.2 Deformation prediction based on fiducial markers registration

Based on the observation that LAHNCs are mostly surrounded by soft tissue, the shape prediction process is formulated as a problem of finding the smoothest force distribution on the tumor surface. Throughout computation, displacement constraints induced by FMs are satisfied, and assumption of no external force on interior nodes is made. The objective function is quadratic in nodal displacement vector x, and thus allows for fast optimization process. The force-field Laplacian energy-minimization problem is formulated as follows:

$$\underset{x}{\operatorname{argmin}}\,x^TK^*x\;\text{ subject to }\begin{cases}Dx=d\\K_lx=0\end{cases}\quad;\quad K^*=(MLK_u)^T(MLK_u) \tag{3}$$

where f_u is the force vector (surface nodes), L is Laplacian matrix, M is inverse mass matrix, K_u is upper stiffness matrix (surface nodes), D is binary indicator matrix, d is measured displacements of FMs, K_l is lower stiffness matrix (interior nodes).

3 RESULTS AND CONCLUSIONS

A deformed version of original tumor reconstruction is created with smoothly distributed force field on the tumor surface. The maximum displacement is equal to 10% of the tumor's longest dimension (Fig. 1(a)). Optimal configuration of laser fibers is generated based on the non-deformed tumor shape (Fig. 1(b)). The same configuration is applied to the deformed tumor.

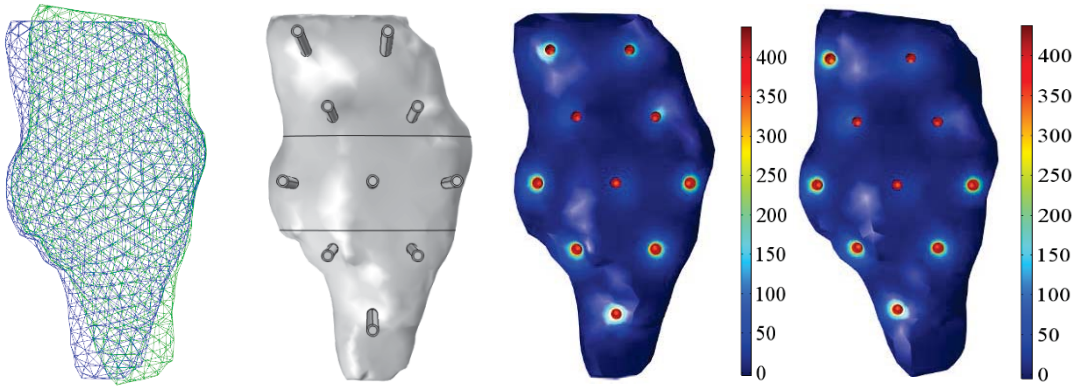

Figure 1: (a) Non-deformed (blue) in comparison with deformed tumor (green). (b) Optimal configuration of laser fibers computed from light propagation modeling. (c) Light-dose distribution according to preplanned fiber configuration on the non-deformed tumor. (d) Light-dose distribution after the tumor has been deformed while maintaining the same light fiber configuration.

According to the simulation results, an overall maximum of 3% less volume of the deformed tumor received the prescribed light dose when compared to the non-deformed tumor model (Fig. 2). A significant local difference is observed at the tumor margins (Fig. 1(c)(d)).

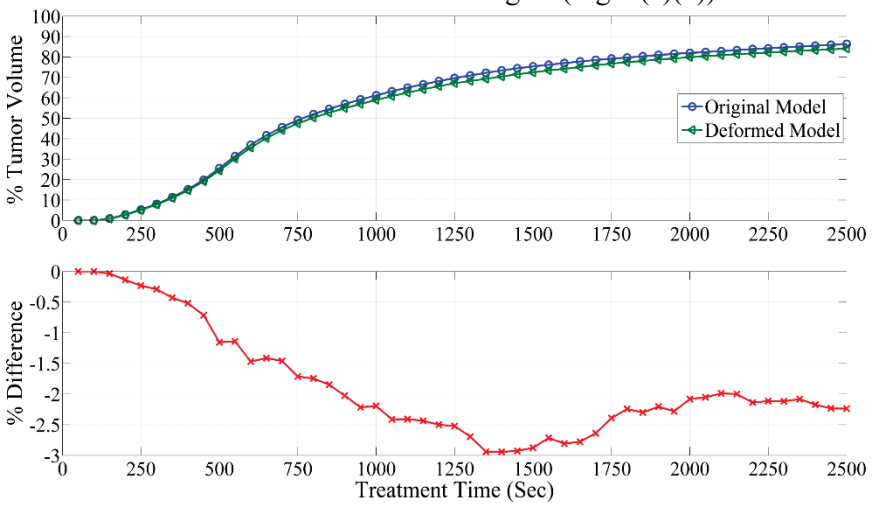

Figure 2: Dose volume histogram (% tumor volume that receives light dose > 100 J/cm²).

By applying the deformation prediction method described in Section 2.2, the deformed tumor shape is reconstructed with a maximum prediction error of 0.7 mm (Fig. 3). The reconstruction process takes less than 6s when performed on an x64 machine with 2.7 GHz Intel i7 processor and 16GB of 1600MHz DDR3L onboard memory.

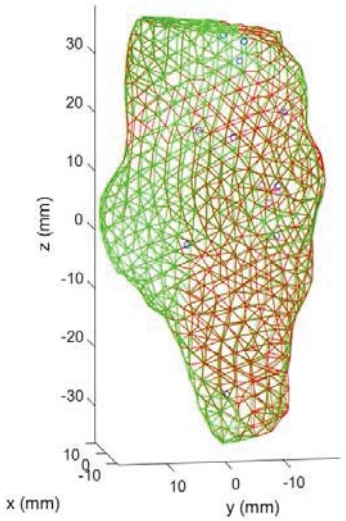

Figure 3: Deformed shape(green) vs predicted shape(red).

In summary, this study shows that (i) an overall maximum of 3% treatment defect (tumor volume that does not receive prescribed light dose) could happen in I-PDT, when the tumor is under deformation of 10% of its longest dimension, (ii) by tracking the position of implanted FMs, the deformed tumor shape can be reconstructed with high fidelity using our deformation prediction method, and (iii) real-time prediction of the tumor's deformed shape can be achieved by using our method on standard personal computer, which demonstrates this study's potential relevance for clinical applications.

4 ACKNOWLEDGEMENT

This study has been supported in part by seeds funds from the Department of Mechanical Engineering at Carnegie Mellon University to Y. Rabin and L.B. Kara; NCI grants R01 CA193610 to G. Shafirstein; P01CA55791 to S. Gollnick; and Roswell Park Cancer Institute Support Grant P30 CA16056.

REFERENCES

[1] Oakley, E., Wrazen, B., Bellnier, D. A., Syed, Y., Arshad, H., and Shafirstein, G., 2015, "A New Finite Element Approach for Near Real-Time Simulation of Light Propagation in Locally Advanced Head and Neck Tumors," Lasers Surg. Med., **47**(1), pp. 60–67.

[2] Patterson, M. S., Chance, B., and Wilson, B. C., 1989, "Time resolved reflectance and transmittance for the non-invasive measurement of tissue optical properties," Appl. Opt., **28**(12), pp. 2331–2336.

[3] Madsen, S. J., Wilson, B. C., Patterson, M. S., Park, Y. D., Jacques, S. L., and Hefetz, Y., 1992, "Experimental tests of a simple diffusion model for the estimation of scattering and absorption coefficients of turbid media from time-resolved diffuse reflectance measurements," Appl. Opt., **31**(18), pp. 3509–3517.

[4] Brodin, N. P., Guha, C., and Tomé, W. A., 2015, "Photodynamic Therapy and Its Role in Combined Modality Anticancer Treatment," Technol. Cancer Res. Treat., **14**(4), pp. 355–368.

[5] Jäger, H. R., Taylor, M. N., Theodossy, T., and Hopper, C., 2005, "MR imaging-guided interstitial photodynamic laser therapy for advanced head and neck tumors," AJNR Am. J. Neuroradiol., **26**(5), pp. 1193–1200.

[6] Lou, P.-J., Jäger, H. R., Jones, L., Theodossy, T., Bown, S. G., and Hopper, C., 2004, "Interstitial photodynamic therapy as salvage treatment for recurrent head and neck cancer," Br. J. Cancer, **91**(3), pp. 441–446.

[7] Wong, K. C. L., Summers, R., Kebebew, E., and Yao, J., 2014, "Tumor Growth Prediction with Hyperelastic Biomechanical Model, Physiological Data Fusion, and Nonlinear Optimization," Medical Image Computing and Computer-Assisted Intervention – MICCAI 2014, P. Golland, N. Hata, C. Barillot, J. Hornegger, and R. Howe, eds., Springer International Publishing, pp. 25–32.

[8] Clatz, O., Sermesant, M., Bondiau, P.-Y., Delingette, H., Warfield, S. K., Malandain, G., and Ayache, N., 2005, "Realistic Simulation of the 3D Growth of Brain Tumors in MR Images Coupling Diffusion with Biomechanical Deformation," Ieee Trans. Med. Imaging, **24**(10), pp. 1334–1346.

[9] Chen, X., Summers, R., and Yao, J., 2011, "FEM-Based 3-D Tumor Growth Prediction for Kidney Tumor," IEEE Trans. Biomed. Eng., **58**(3), pp. 463–467.

[10] Kamrani, A., and Azimi, M., 2014, "Geometrical analysis and predictive modeling of head and neck tumors," 2014 World Automation Congress (WAC), pp. 1–5.

[11] Gill, S., Li, J., Thomas, J., Bressel, M., Thursky, K., Styles, C., Tai, K. H., Duchesne, G. M., and Foroudi, F., 2012, "Patient-reported complications from fiducial marker implantation for prostate image-guided radiotherapy," Br. J. Radiol., **85**(1015), pp. 1011–1017.

[12] Ng, M., Brown, E., Williams, A., Chao, M., Lawrentschuk, N., and Chee, R., 2014, "Fiducial markers and spacers in prostate radiotherapy: current applications," BJU Int., **113**, pp. 13–20.

[13] Cendales, R., Torres, F., Arbelaez, J., Gaitan, A., Vasquez, J., and Bobadilla, I., 2015, "Displacements of fiducial markers in patients with prostate cancer treated with image guided radiotherapy: A single-institution descriptive study," Rep. Pract. Oncol. Radiother., **20**(1), pp. 38–42.

[14] Bathe, K.-J., 1996, Finite Element Procedures, Prentice Hall.

[15] Rosenberg, S., 1997, The Laplacian on a Riemannian Manifold: An Introduction to Analysis on Manifolds, Cambridge University Press, Cambridge.